BIOCHEMISTRY
including biophysical chemistry & molecular biology

ARTICLE

pubs.acs.org/biochemistry

Transmembrane Topology of Mammalian Planar Cell Polarity Protein Vangl1

Alexandra Iliescu, Michel Gravel, Cynthia Horth, Sergio Apuzzo, and Philippe Gros*

Department of Biochemistry and Complex Traits Program, McGill University, Montreal, Quebec, Canada H3G 0B1

Supporting Information

ABSTRACT: Vangl1 and Vangl2 are membrane proteins that play an important role in neurogenesis, and Vangl1/Vangl2 mutations cause neural tube defects in mice and humans. At the cellular level, Vangl proteins regulate the establishment of planar cell polarity (PCP), a process requiring membrane assembly of asymmetrically distributed multiprotein complexes that transmit polarity information to neighboring cells. The membrane topology of Vangl proteins and the protein segments required for structural and functional aspects of multiprotein membrane PCP complexes is unknown. We have used epitope tagging and immunofluorescence to establish the secondary structure of Vangl proteins, including the number, position, and polarity of transmembrane domains. Antigenic hemagglutinin A (HA) peptides (YYDVPDYS) were inserted in predicted intra- or extracellular loops of Vangl1 at positions 18, 64, 139, 178, 213, and 314, and individual mutant variants were stably expressed at the membrane of MDCK polarized cells. The membrane topology of the exofacial HA tag was determined by a combination of immunofluorescence in intact (extracellular epitopes) and permeabilized (intracellular epitopes) cells and by surface labeling. Results indicate that Vangl proteins have a four-transmembrane domain structure with the N-terminal portion (HA18 and HA64) and the large C-terminal portion (HA314) of the protein being intracellular. Topology mapping and hydropathy profiling show that the loop delineated by TMD1−2 (HA139) and TMD3−4 (HA213) is extracellular while the segment separating predicted TMD2−3 (HA178) is intracellular. This secondary structure reveals a compact membrane-associated portion with very short predicted extra- and intracellular loops, while the protein harbors a large intracellular domain.

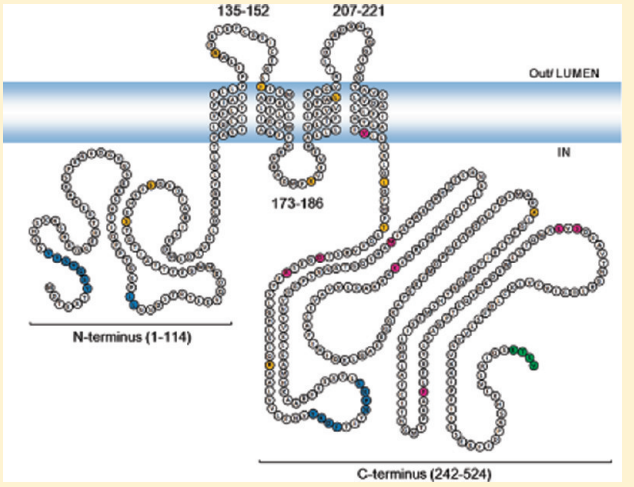

Neural tube defects (NTDs) are a group of common congenital malformations in humans that arise from a partial or complete failure of the neural tube to close during embryogenesis. Complex genetic and environmental factors are known to be important etiological factors in the emergence of NTDs in humans.[1] The complex genetic component has been difficult to decipher in humans but has been studied in naturally occurring and experimentally induced mouse mutants.[2,3] The *loop−tail* (*Lp*) mouse is an accepted model for the study of NTDs.[4,5] Heterozygous *Lp* mice are normal except for a characteristic "looped" tail, while homozygote *Lp*/*Lp* embryos die in utero of a severe form of NTD, craniorachischisis, in which the neural tube remains open from hindbrain to the most caudal extremity of the developing embryo. Three *Lp* alleles have been described so far (*Lp*, Lp^{m1Jus}, and Lp^{m2Jus}), and we have shown that the NTD in these three allelic variants is caused by independent loss-of-function mutations (D255E, R259L, and S464N) in the *Vangl2* gene.[6,7] In mammals, there are two *Vangl* genes, *Vangl1* and *Vangl2*. These two genes encode proteins that are expressed during embryogenesis and show complementary patterns of expression in the developing neural tube. Their expression persists postnatally in certain tissues; however, *Vangl2* is expressed abundantly and broadly in the dorsal and ventral portions of the neural tube, prior to, during, and after closure (E7.5−E11.5), while *Vangl1* expression is mostly restricted to the ventral portion of the neural tube and to the notochord.[8,9] *Vangl1* and *Vangl2* genetically interact during neural tube formation, and animals doubly heterozygous for *Vangl1* and *Vangl2* mutations ($Vangl1^{\pm}$:$Vangl2^{\pm}$) show craniorachischisis.[10] Importantly, we[11−13] and others[14] have subsequently identified loss-of-function mutations in the human *VANGL1* and human *VANGL2* genes in familial and sporadic cases of neural tube defects in humans.

Mammalian *Vangl* genes are relatives of the *Drosophila Van Ghog/Strabismus* (*Vang/Stbm*) gene, a member of the so-called planar cell polarity (PCP) gene family. In flies, this family also includes *Frizzled* (*Fz*), *Diego* (*Dgo*), *Flamingo* (*Fmi*), *Prickle* (*Pk*), and *Dishevelled* (*Dvl*). Mutations in these genes alter the establishment of planar cell polarity, which causes a number of abnormalities in the fly, including

Received: November 3, 2010
Revised: January 28, 2011
Published: February 03, 2011

Table 1. Oligonucleotides Used for Epitope Insertion by Site-Directed Mutagenesis

1HA18	NT	K18[a]	F	TAC CCA TAC GAT GTG CCA GAC TAC GCT agc aaa tct cac aga caa ggg gaa aga act aga
			R	gct AGC GTA GTC TGG CAC ATC GTA TGG GTA ttt cga atg act tga ata gta aga ata tcc
2HA64	NT	T64[a]	F	TAC CCA TAC GAT GTG CCA GAC TAC GCT agc gag gaa gtt cag gat gac aac tgg gga gag
			R	gct AGC GTA GTC TGG CAC ATC GTA TGG GTA tgt ccg agt aga atc att tcc caa cag ggg
3HA139	TMD1−2	R139[a]	F	TAC CCA TAC GAT GTG CCA GAC TAC GCT agc gat gag ctg gag cct tgt ggc aca att tgt
			R	gct AGC GTA GTC TGG CAC ATC GTA TGG GTA cct cca cag gat cgg agg taa aag gat gaa
4HA178	TMD2−3	D178[a]	F	TAC CCA TAC GAT GTG CCA GAC TAC GCT agc atg cca cgg gtg ttt gtg ttt cgt gcc ctt
			R	gct AGC GTA GTC TGG CAC ATC GTA TGG GTA gtc agc tct ccg ctt gcg gaa aaa aag tgc
5HA213	TMD3−4	D213[a]	F	TAC CCA TAC GAT GTG CCA GAC TAC GCT agc cgg aat tac cag ggc att gtg caa tat gca
			R	gct AGC GTA GTC TGG CAC ATC GTA TGG GTA gtc ccg aga gtc caa aat gcg gac ccc gta
6HA314	CT	V314[a]	F	TAC CCA TAC GAT GTG CCA GAC TAC GCT agc gat ggc ccc agt aac aat gcc act ggc cag
			R	gct AGC GTA GTC TGG CAC ATC GTA TGG GTA tac att gta gac ttt cag ccc ggc cat atg

[a] Amino acid residue immediately preceding the site of insertion of the HA epitope. The HA epitope nucleotide sequence is in uppercase.

the orientation of the eye (omatidiae) and hair bristles on the wings and legs.[15,16] In the fly, the redistribution and asymmetric positioning of membrane-bound Dvl−Fz and Vang−Pk complexes in epithelial cells are believed to propagate a polarity signal essential for PCP organization of cell layers.[17−19] The PCP pathway has been conserved in mammals, and a clear example is the precise orientation of the stereociliary bundles of the neurosensory epithelium of the inner ear. In the mouse, inactivating mutations in PCP genes *Vangl1* or *Vangl2*, *Dsh* (*Dvl*), and *Fmi* (*Celsr1*) cause disruption of these structures in the inner ear.[20] In addition, vertebrate relatives of fly PCP genes regulate convergent extension movements during embryogenesis, including the narrowing and lengthening of the neural plate required for neural tube closure, and mutations in *Vangl2* (*Lp*),[6] *Vangl1*/*Vangl2*,[10] *Dvl1*/*2*,[21] *Dvl2*/*3*,[22] *Celsr1*,[23] and *Fz3*/*6*[24,25] cause craniorachischisis.

Mammalian Vangl proteins are composed of 521−526 amino acids. Subcellular localization studies by immunofluorescence and cell fractionation studies have shown that Vangl proteins are integral membrane proteins, both in primary tissues In Vivo and in transfected cultured cells in vitro.[19,26,27] Plasma membrane (PM) targeting of Vangl proteins is essential for function, and we have shown that *Lp*-associated pathological mutations in Vangl2 impair PM localization of the protein.[27] Vangl membrane targeting is also required for interaction with other PCP proteins, including Dvl.[28] The secondary structure of Vangl proteins, including its membrane topology, has not been established, and this information is required for understanding how Vangl proteins interact with other PCP proteins to assemble membrane-bound polarity signaling complexes. Multiple-sequence alignments and hydropathy profiling have predicted at least three and possibly four TM domains in the amino-terminal half of the protein, with the carboxy-terminal portion encoding a large hydrophilic domain. This highly conserved carboxy half of the protein is responsible for physical interaction with cytoplasmic Dvl proteins (Dvl1, Dvl2, and Dvl3),[28] possibly though a PDZ binding motif (ETSV tetrapeptide) located at its carboxy-terminal extremity. This strongly suggests that the carboxyl half of Vangl proteins is intracellular.

In this study, we have used epitope tagging to establish the secondary structure of Vangl proteins, including the number, position, and polarity of transmembrane domains. The membrane topology of the hemagglutinin HA tags inserted in different locations of the protein was determined by a combination of immunofluorescence in intact (extracellular epitopes) and permeabilized (intracellular epitopes) cells and was verified by surface labeling. Results from these studies were unambiguous and established a four-TM domain topology for Vangl proteins with the amino and carboxy termini located on the intracellular side of the membrane.

EXPERIMENTAL PROCEDURES

Material and Antibodies. Geneticin (G418) and penicillin/streptomycin were purchased from Invitrogen (Carlsbad, CA). Restriction endonucleases were from New England Biolabs (Ipswich, MA), and Taq DNA polymerase was from Invitrogen. The mouse monoclonal antibodies directed against the influenza hemagglutinin epitope (HA.11) were purchased from Covance (Berkeley, CA). The mouse monoclonal antibody recognizing Na,K-ATPase (α) was from Santa Cruz Biotechnology (Santa Cruz, CA). Cy3-conjugated goat anti-mouse antibody and peroxidase-coupled goat anti-mouse antiserum were from Jackson ImmunoResearch Laboratories (West Grove, PA).

Plasmids and Site-Directed Mutagenesis. The human *VANGL1* cDNA was used as a template for the construction of all mutants. The cDNA was amplified from total human RNA by reverse transcriptase polymerase chain reaction (RT-PCR) and cloned into the pCS2+ plasmid vector. PCR-mediated mutagenesis with overlapping oligonucleotides was used to insert a short antigenic peptide epitope (EQKLISEEDL) from the human c-Myc protein at the N-terminus of VANGL1 as we have previously described, followed by cloning into the pCB6 mammalian expression vector. For the transmembrane domain topology mapping analysis, hemagglutinin (HA) epitopes (YPYDVPDYA) were inserted in predetermined positions in the protein by recombinant PCR, using mutagenic oligonucleotide primers listed in Table 1. To allow potential insertion of additional contiguous HA epitope(s) at these positions, a NheI restriction site was engineered at the 3′-end of each HA sequence, accounting for the additional Ser residue found at the end of the HA tag. To facilitate identification of transfected cells expressing various recombinant hVANGL1 proteins, c-Myc/HA-tagged h*VANGL1* cDNAs were fused in-frame to the green fluorescent protein (GFP) by cloning into the peGFP-C1 vector (Clontech, Mountain View, CA). The integrity of all *VANGL1* cDNA constructs was verified by nucleotide sequencing.

Cell Culture, Transfection, and Western Blotting. Madin-Darby canine kidney (MDCK) epithelial cells were grown in Dulbecco's modified Eagle's medium (DMEM) supplemented with 10% fetal bovine serum (FBS), 100 units/mL penicillin, and 100 μg/mL streptomycin (37 °C, 5% CO_2). To generate stable transfectants, MDCK cells were transfected with c-Myc/HA-tagged VANGL1 constructs subcloned in peGFP-C1 using Lipofectamine Plus Reagent

as described in the manufacturer's instructions (Invitrogen). Selection for stably transfected clones was conducted in growth medium containing 0.3 mg/mL G418 for 10−14 days. Expression of recombinant c-Myc/HA-tagged GFP-VANGL1 was initially identified by fluorescence microscopy on live cells and confirmed by Western blotting analysis. Total cell lysates were prepared in RIPA buffer [50 mM Tris-HCl (pH 7.5), 150 mM NaCl, 5 mM EDTA, 1% Triton X-100, and 0.1% sodium dodecyl sulfate (SDS) supplemented with protease inhibitors] and cleared by being passed through a 25 gauge needle and by centrifugation at 13000*g* for 10 min (4 °C). Whole cell extracts (50 μg) were separated by electrophoresis using 7.5% SDS−polyacrylamide gels, followed by electroblotting and incubation with the monoclonal anti-HA antibody (HA.11) (used at 1:1000). Immune complexes were revealed with a horseradish peroxidase-conjugated goat anti-mouse antibody (1:10000) and visualized by enhanced chemiluminescence (SuperSignal West Pico kit, Thermo Scientific, Rockford, IL).

Immunofluorescence and Confocal Microscopy. Stably transfected MDCK cell clones expressing individual HA-tagged VANGL1 proteins were seeded at high density onto glass coverslips in a 24-well plate. Forty-eight hours later, cells were washed twice with ice-cold PBS, fixed for 15 min in 4% paraformaldehyde (PFA) in PBS, and then permeabilized with 0.1% Triton X-100 in PBS for 15 min. After being blocked for nonspecific binding with 5% goat serum and 0.1% bovine serum albumin (BSA) in PBS for 1 h, the cells were incubated with the desired primary antibody [mouse anti-Na,K-ATPase (1:50) or mouse anti-HA (1:200)] for 1 h and washed three times with 0.1% BSA in PBS. Finally, the coverslips were incubated for 1 h with the goat anti-mouse Cy3 secondary antibody (1:1000) and washed three times with 0.1% BSA in PBS. All the incubations were conducted at room temperature, and the antibodies were all diluted in blocking solution. To detect cell surface expression of the HA epitope under nonpermeabilized conditions, MDCK cells expressing HA-tagged VANGL1 variants were incubated with the mouse anti-HA (1:200) antibody in DMEM containing 2% nonfat milk for 2 h at 37 °C. After several washes with PBS, cells were fixed for 15 min with 4% PFA in PBS and incubated with goat anti-mouse Cy3 antibody (1:1000) for 1 h. For immunofluorescence, coverslips were rinsed twice with PBS and once in water and mounted using Permafluor Aqueous Mounting Medium (Thermo Scientific, Fremont, CA). Confocal microscopy was conducted with a Zeiss LSM5 Pascal laser scanning confocal microscope. All image analyses were performed using LSM5 Image. To maximize image quality, a Median filter (3 × 3) was applied to the images using Image-Pro.

Estimation of Cell Surface Expression by an Enzyme-Linked Immunosorbent Assay. The cell surface expression of HA-tagged VANGL1 proteins was estimated using an enzyme-linked immunosorbent assay (ELISA), as described previously[27] with the following modifications. Briefly, MDCK cells stably expressing HA-tagged VANGL1 variants were seeded at confluence in 24-well plates and grown for 4 days. Cells were then washed with PBS and incubated in Ca^{2+}-free DMEM for 20 min, prior to incubation with 10 mM EGTA for 5 min. To evaluate the expression of HA-tagged VANGL1 proteins at the cell surface, cells were incubated with mouse anti-HA antibody (1:200 in Ca^{2+}-free DMEM) for 2 h (37 °C, 5% CO_2). Cells were washed, fixed with 4% PFA in PBS for 15 min, and incubated with HRP-conjugated goat anti-mouse antibody (1:4000 in a 5% nonfat milk/PBS mixture for 1 h). To evaluate total HA-tagged VANGL1 variants, cells were fixed after the EGTA treatment, permeabilized with 0.1% Triton X-100 in PBS for 30 min, and blocked in a 5% nonfat milk/PBS mixture. Cells were then incubated with anti-HA antibody (1:200 in blocking solution) for 1 h, washed, and incubated with HRP-conjugated goat anti-mouse antibody (1:4000 in blocking solution). Peroxidase activity was quantified colorimetrically using the HRP substrate [0.4 mg/mL *O*-phenylenediamine dihydrochloride (OPD) (Sigma-Aldrich)] according to the manufacturer's instructions. The reaction was stopped via addition of 3 N HCl; absorbance readings (490 nm) were taken in an ELISA plate reader, and the background absorbance reading from the nonspecific binding of the primary antibody to vector-transfected cells was subtracted for each sample. Cell surface readings were normalized to the total HA-tagged GFP-VANGL1 value for each cell clone and were expressed as a percentage.

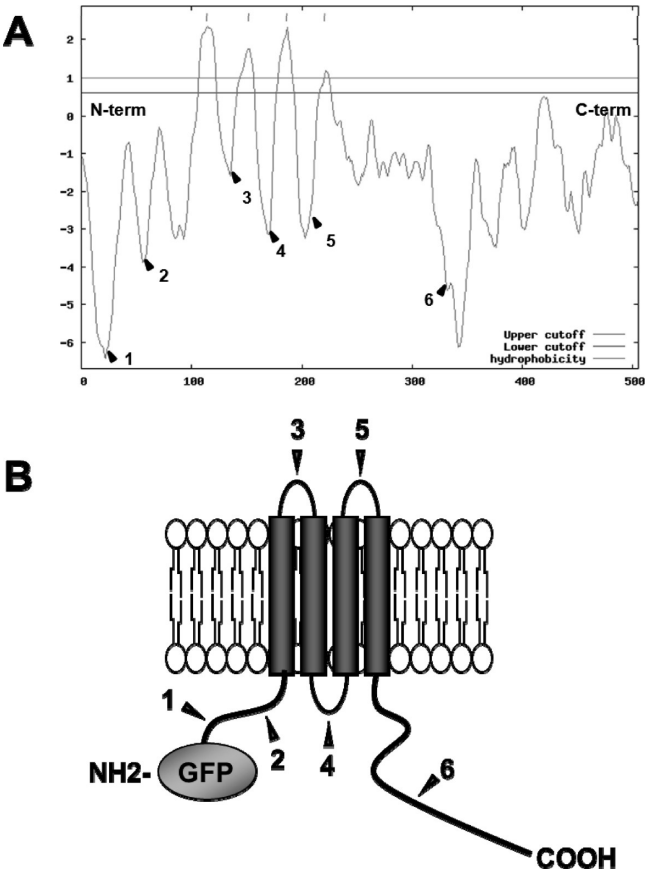

Figure 1. Construction of VANGL1 proteins containing hemagglutitin (HA) epitope tags. The sites for insertion of YPYDVDYA hemagglutinin (HA) epitopes into individual VANGL1 proteins are indicated (black arrowheads), along with the numerical designation of the construct (NT, 1−6, CT). (A) These have been superimposed on the hydropathy plot of VANGL1 protein produced by TOPPRED2 using a 20-residue sliding window (core window, 12 residues; wedge windows, 4 residues). The default parameters suggested for predicting the presence of TMDs in eukaryotic proteins were used, such as the GES cutoff values (lower 0.6, putative; upper 1.0, certain). (B) Two-dimensional model of the Vangl1 protein with the inserted HA tags at various positions.

RESULTS

Epitope-Tagged Mutant VANGL1 Constructs. Hydropathy profiling and analysis of hydrophobic segments of the predicted amino acid sequence of the human VANGL1 protein using the TOPPRED software package are shown in Figure 1. According to this analysis, hVANGL1 shows four predicted transmembrane domains in the amino-terminal half of the protein. Using a predicted length of 20 amino acids and via minimization of the number of charges to be included in the transmembrane portion, the four TM domains are

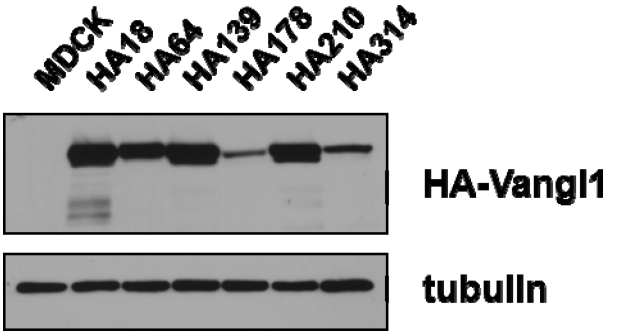

Figure 2. Expression of HA epitope-tagged VANGL1 constructs in MDCK cells. MDCK cells were stably transfected with GFP-h*VANGL1* cDNA constructs modified by the addition of individual HA epitopes (HA18, HA64, HA139, HA178, HA213, and HA314) and inserted into mammalian expression vector pCB6. Total cell lysates (50 μg per lane) were prepared, resolved by electrophoresis on a 7.5% SDS−polyacrylamide gel, and analyzed by Western blotting using a mouse monoclonal anti-HA.11 epitope antibody.

predicted to span segments of residues 114−134 (TM1), 152−172 (TM2), 186−206 (TM3), and 222−242 (TM4). In addition, we also used the TMHMM predictive program, and both the probability plot and comparison with TOPPRED are shown in Figure S1 of the Supporting Information. The amino acid sequence of all four predicted TMs is highly conserved among Vangl relatives from mouse, human, zebrafish, worm, and flies with 8 of 20 (TM1), 5 of 20 (TM2), 14 of 20 (TM3), and 17 of 20 (TM4) highly conserved positions (defined as >7 of 9 sequences identical at that position), suggesting that these domains play an important conserved role in the function of these Vangl relatives. However, TM4 consistently gives lower scores in predictive programs than the three other TM domains. In addition, there is a predicted N-linked glycosylation site (N-X-S/T) in the amino terminus of the protein that is well conserved among Vangl relatives, thereby arguing against a four-TM model with the amino and carboxy termini of the protein being intracytoplasmic.

To determine the membrane topology of VANGL1, including the number and position of individual TM domains, as well as the cytoplasmic versus extracytoplasmic location of the amino and carboxy termini, we used an epitope tagging method.[29] In this method, antigenic hemagglutinin HA epitope tags (YPYDVPDYAS) are inserted in strategic positions of the protein in individual mutants, followed by expression of the HA-tagged protein at the plasma membrane of transfected cells and determination of the polarity of the exofacial tag by immunofluorescence in intact (extracellular) and permeabilized cells (intracellular). This method provides topological data about proteins that are properly expressed at the plasma membrane in a functional state. HA epitopes were inserted at two positions of the amino terminus (positions 18 and 64; NT constructs) and at position 314 in the carboxy-terminal portion (CT construct). Three additional HA tags were inserted at positions 139, 178, and 213. These positions correspond to peak hydrophilic segments [from hydropathy profiling (Figure 1A)] in the otherwise hydrophobic moiety of the protein, and therefore possibly corresponding to short intra- or extracytoplasmic loops delineated by TM1−TM2 (139), TM2−TM3 (178), and TM3−TM4 (213) intervals (Figure 1).

Expression of Epitope-Tagged VANGL1 Mutants in Transfected MDCK Kidney Cells. All tagged *VANGL1* cDNA constructs were transfected into MDCK cells, and the expression of the resulting HA-tagged VANGL1 proteins was initially detected by GFP fluorescence in intact cells and subsequently verified by immunoblotting. Representative immunoblots using an anti-HA monoclonal antibody are shown for single cell clones expressing individual mutant VANGL1 proteins (Figure 2). The MDCK cell line was chosen as a recipient in transfection experiments because it is derived from a cell lineage (kidney tubular epithelium) that normally expresses Vangl proteins In Vivo. Briefly, we could obtain stable transfectants expressing robust levels of VANGL1 for constructs 18, 64, 139, and 213, while lower levels of expression were consistently noted in cell clones expressing constructs 178 and 314 (Figure 2). The recombinant

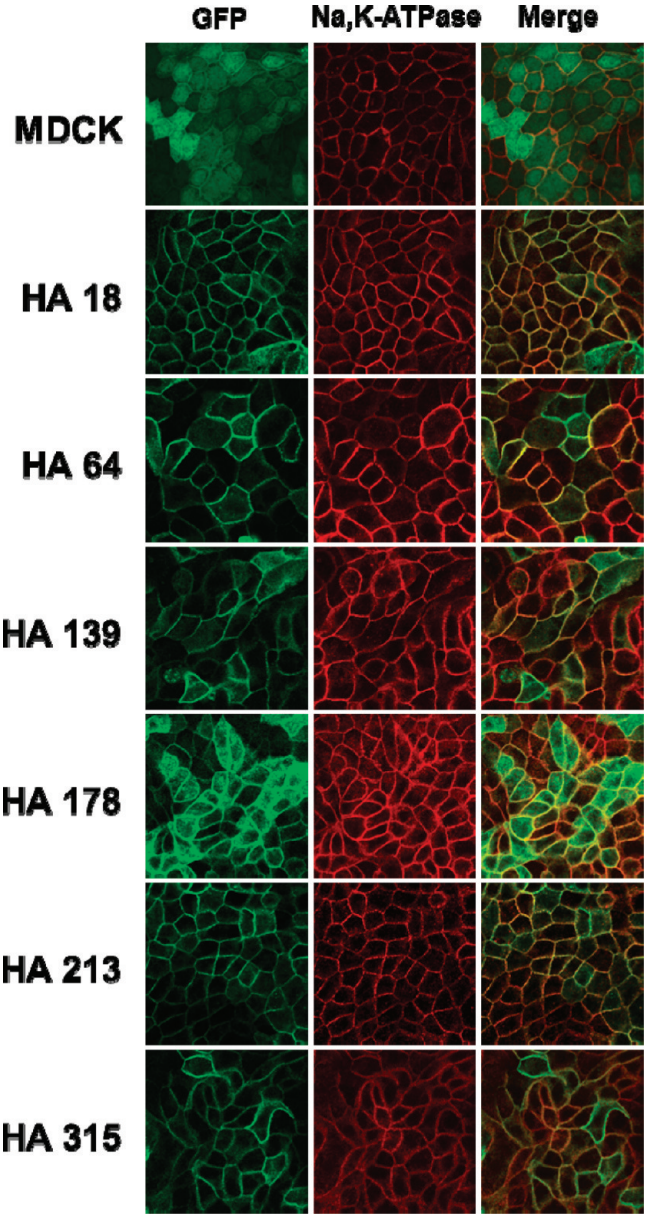

Figure 3. Cellular localization of HA epitope-tagged VANGL1 proteins transfected in MDCK cells. Transfected MDCK cells stably expressing GFP alone or the different GFP-*VANGL1* constructs (green) containing single HA epitope tags (HA18, HA64, HA139, HA178, HA213, and HA314) were grown to confluence, fixed, permeabilized, stained for Na,K-ATPase followed by Cy3-conjugated secondary antibody (red), and examined by confocal microscopy. The merged images show that the majority of GFP-tagged VANGL1-HA constructs are associated with the plasma membrane and colocalize with Na,K-ATPase (yellow). Images are representative of at least three independent experiments.

dx.doi.org/10.1021/bi101767a |*Biochemistry* 2011, 50, 2274–2282

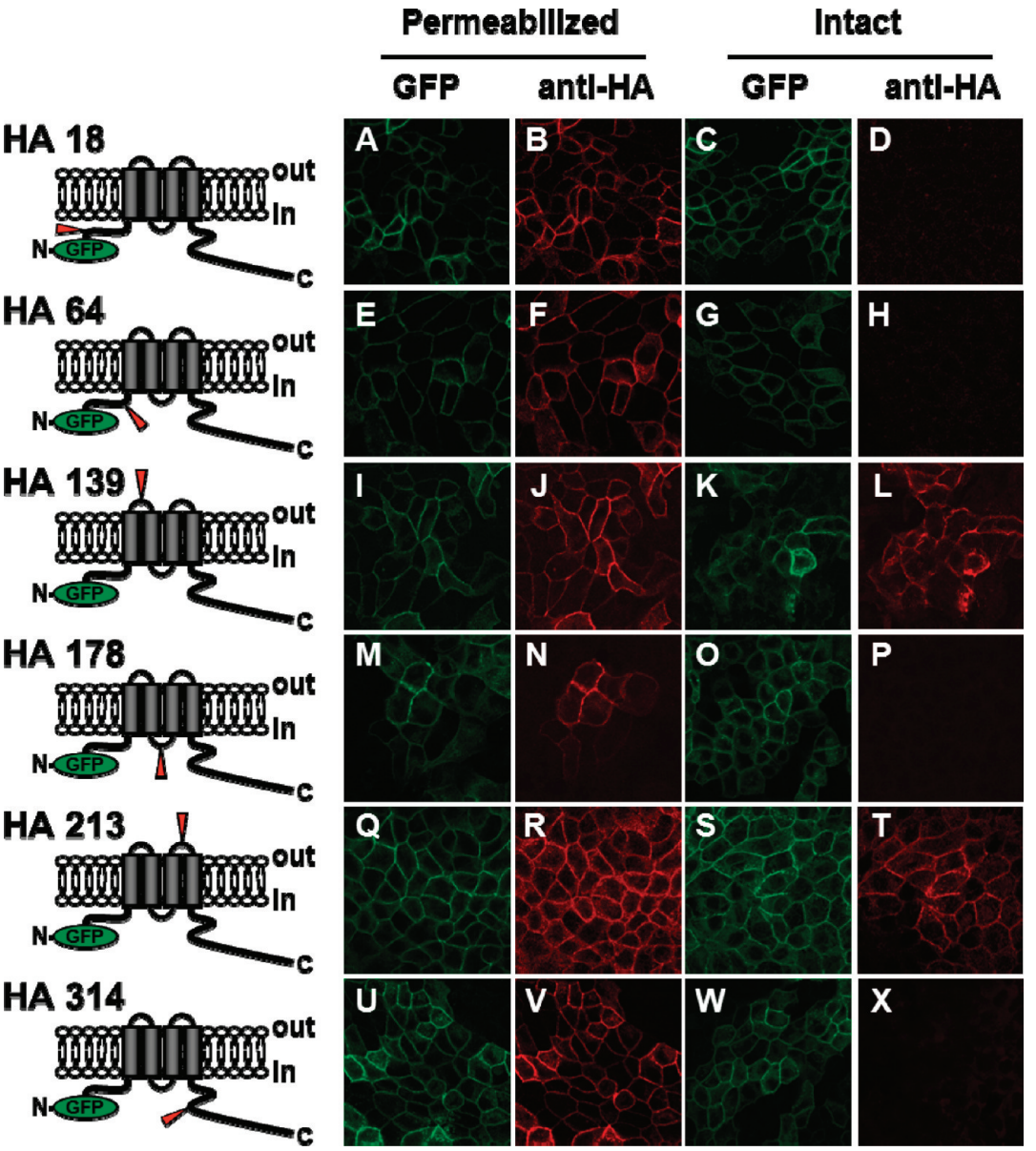

Figure 4. Immunofluorescence analysis of HA epitope-tagged VANGL1 proteins in intact and permeabilized cells. MDCK cells stably expressing individual HA-tagged VANGL1 proteins were analyzed by immunofluorescence. A schematic representation of the VANGL1 proteins with the position (HA18, HA64, HA139, HA178, HA213, and HA314) of the inserted HA tag (red arrows) is shown at the left. Immunofluorescence was assessed with the mouse monoclonal anti-HA epitope antibody (HA.11) on cells either untreated (intact cells, right two columns) or permeabilized with 0.1% Triton X-100 (permeabilized, left two columns). Cells were then incubated with Cy3-conjugated secondary goat anti-mouse antibody, and images were acquired by confocal microscopy. The HA epitopes in MDCK cells expressing HA139 (I−L) and HA213 (Q−T) were detected in intact and permeabilized cells (extracytoplasmic), while cells expressing HA18 (A−D), HA64 (E−H), HA178 (M−P), and HA314 (U−X) were detected only in permeabilized cells (intracytoplasmic). GFP fluorescent images (columns 1 and 4) were used as controls. Images are representative of at least three independent experiments.

proteins were detected as immunoreactive bands of ~80 kDa in agreement with the predicted size of the VANGL1 protein backbone (~55 kDa) fused to GFP (27 kDa).

The subcellular localization of GFP-HA VANGL1 proteins was analyzed by confocal microscopy. As opposed to the cytoplasmic fluorescence signal detected in MDCK cells expressing only control GFP (Figure 3), GFP-VANGL1 MDCK transfectants exhibited strong localization of the GFP fluorescence at the membrane (Figure 3, middle panels), producing a typical meshlike signal in confluent cell monolayers. In addition, the GFP-VANGL1 signal was found to fully colocalize with Na,K-ATPase, a specific marker for the basolateral membrane of MDCK cells (Figure 3, middle panels). Taken together, results in Figure 3 show that all GFP-tagged VANGL1 constructs are expressed at the basolateral membrane of MDCK cells, indicating that none of the HA tag insertions affect the maturation or membrane targeting of the protein.

Membrane Topology of the Inserted HA Epitope Tags. The intra- or extracytoplasmic localization of the HA tags was assessed for each construct by immunofluorescence analysis of the corresponding MDCK transfectant using the anti-HA monoclonal antibody (Figure 4 and Figure S2 of the Supporting Information). Immunofluorescence was performed in parallel on intact cells to

dx.doi.org/10.1021/bi101767a |*Biochemistry* 2011, 50, 2274–2282

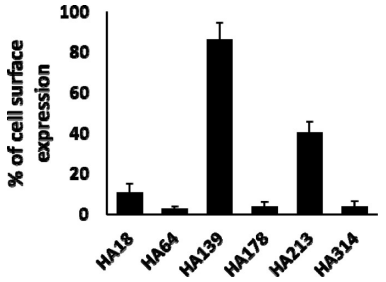

Figure 5. Detection of HA epitope-tagged proteins by surface labeling. MDCK cells stably expressing individual HA-tagged VANGL1 proteins were incubated with anti-HA antibody with or without prior permeabilization with 0.1% Triton X-100 treatment, followed by incubation with HRP-coupled secondary antibody. The amount of bound secondary antibody was determined by a colorimetric assay using the HRP substrate *o*-phenylenediamine dihydrochloride (OPD) measured at 490 nm. The presence of HA-tagged VANGL1 expressed at the cell surface (in intact cells) is shown as a fraction of total protein expression (in permeabilized cells) normalized for nonspecific binding of the secondary antibody alone in each individual clone. Error bars represent standard errors of the mean of at least four independent experiments (in quadruplicate).

detect extracytoplasmic tags and in cells permeabilized with detergent to detect tags present on the intracytoplasmic face of the membrane. For all MDCK transfectants, GFP fluorescence images were also acquired for the identification of the position of cells examined by immunofluorescence with the anti-HA antibody. Strong fluorescent signals were observed in both intact and permeabilized cells for constructs 139 (TMD1−2) and 213 (TMD3−4), suggesting that these corresponding segments of VANGL1 are extracytoplasmic. Conversely, strong fluorescence signals were obtained only under permeabilized conditions for cells transfected with constructs 18 (N-terminus), 64 (N-terminus), 178 (TMD2−3), and 314 (C-terminus), suggesting that the corresponding tagged segments of VANGL1 are intracytoplasmic. For all of the constructs, the polarity of the HA tags was validated by immunofluorescence in multiple independently transfected cell clones.

Validation of HA Epitope Localization in VANGL1. The topology of inserted HA tags established by immunofluorescence was validated by an enzymatic method, which additionally provides an estimative of the amount of exofacial tag expressed at the surface of the cell. For this, MDCK transfectants expressing individual HA-tagged VANGL1 constructs were fixed and incubated with primary anti-HA antibody with (total protein expression) or without (surface protein expression) permeabilization with detergent. The cells were then incubated with a secondary horseradish peroxidase (HRP)-conjugated antibody, and the amount of bound secondary antibody was quantified colorimetrically using HRP substrate *o*-phenylenediamine dihydrochloride (OPD). Results in Figure 5 show the amount of surface expression of each VANGL1-HA construct, presented as a percentage of the total amount of protein expressed in the corresponding clone and measured under permeabilized conditions. MDCK cells transfected with constructs 139 and 213 were found to have a significantly greater proportion of accessible HA-tagged VANGL1 at their surface (87 and 41%, respectively) than constructs 18, 64, 178, and 314 (which had between 3 and 11%). These results are in agreement with immunofluorescence experiments and indicate that the HA tags in constructs 139 and 213 are expressed on the extracytoplasmic side of the membrane, while the HA tags in constructs 18, 64, 178, and 314 are expressed on the intracytoplasmic side of the membrane.

DISCUSSION

To date, *VANGL1* and *VANGL2* are the only genes in which loss-of-function mutations have been associated with neural tube defects in humans. The *Vangl* gene was initially identified in genetic screens in flies for mutations that affect the structure of certain appendages on the wing and legs (hair bristles) and the orientation of the eye unit (omatidiae) structure. This indicates that *Vangl* plays an important role in the orientation of cells in the plane of epithelial structures, a basic process known as planar cell polarity (PCP). In mammals, *Vangl* also regulates the process of convergent extension (CE) movements. CE is critical to the formation of many embryonic structures, including the neural tube and the heart. Little is known about the molecular mechanism of action of Vangl proteins in the establishment of PCP or in the control of CE movements. However, recruitment of Vangl proteins to the plasma membrane is absolutely required for function, and we have shown that *Vangl1/2* mutations affecting PCP of inner ear structures and causing cranioraschischisis in *loop−tail* (*Lp*) mice abrogate membrane expression of the protein.[9,27] Likewise, Vangl proteins can interact with cytoplasmic Dvl,[28] and we have observed that *Lp*-associated *Vangl2* mutations in mice and neural tube defects associated *VANGL1* mutations in humans abrogate interaction with Dvl proteins. However, the protein domains involved in protein−protein interactions in these membrane complexes, in the recruitment of extracellular adhesion molecules to propagate positional information, or in the transmission of intracellular signals are unknown.

As a first step in addressing these issues, we have determined the membrane topology of human VANGL1. For this, we inserted HA epitopes at discrete positions of the membrane-associated portion of the protein. The modified proteins were then expressed in transfected cells, and the membrane topology of the inserted tag was determined by immunofluorescence and surface labeling. For these studies, we chose the MDCK kidney polarized epithelial cell line. Vangl proteins localize at the baso and lateral side of several epithelial cells In Vivo, including bronchial tree, intestinal crypt, sweat glands, and kidney tubules.[9] MDCK is derived from kidney, and we have shown that the Vangl proteins expressed in these cells are targeted to the basal and lateral membrane.[27] Thus, topology data generated from proteins expressed at the basolateral membrane of MDCK cells are likely to reflect the native membrane topology of Vangl proteins in normal tissues. HA epitopes were inserted in the amino terminus at two different positions [18 and 64 (NT constructs)] and at position 314 in the carboxy-terminal portion (CT construct). Three additional HA tags were inserted at positions 139, 178, and 213, which represented peaks of hydrophilicity in the otherwise hydrophobic membrane-associated portion of the protein (based on hydropathy analysis shown in Figure 1). All constructs could be expressed at robust levels in the membrane of MDCK transfectants, suggesting that none of the inserted tags disrupted protein folding and/or membrane targeting. These results suggest that the short predicted intracytoplasmic or extracytoplasmic loops in the membrane regions are solvent-exposed and indeed accessible for binding of the antibody to the tag. Results from epitope mapping studies (immunofluorescence and surface labeling) were unambiguous and demonstrated a four-transmembrane domain structure for VANGL1 with intracellular amino and carboxy termini, including a large intracytoplasmic domain in the C-terminal half downstream of TM4 (Figure 6).

These topology data and associated model established here experimentally for human VANGL1 are most likely applicable to

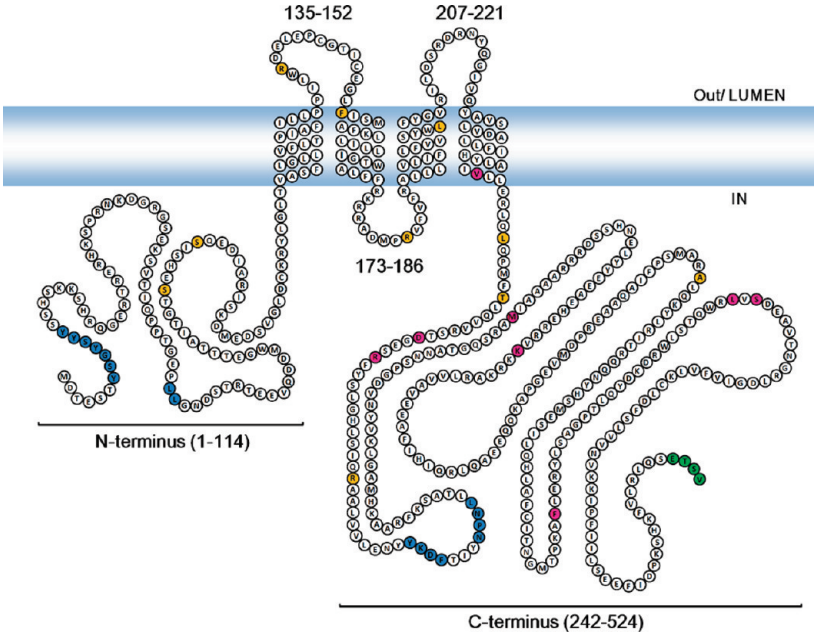

Figure 6. Topological model and structural features of the Vangl protein family. The positions of the four transmembrane domains of the protein as predicted by hydropathy profiling and as established here by epitope mapping are shown. Individual predicted intracellular and extracellular segments and their position in the primary amino acid sequence are shown. Amino acid residues defining sequence landmarks and signature motifs are depicted in different colors, including amino acid variants in Vangl1 and Vangl2 associated with neural tube defects in mice and humans (orange and pink) and in which loss of function has been demonstrated (pink), the ETSV sequence corresponding to a PDZ binding motif (green), and the consensus tyrosine-based and dileucine motifs associated with protein sorting and membrane targeting (blue) (see the text for details). Finally, the polarity of the protein and membrane domains with respect to the membrane (light blue) is indicated (in, out, lumen).

the rest of the Vangl protein family. Indeed, members of the Vangl family share a high degree of sequence similarity, and functional complementation studies in zebrafish mutants (*trilobite*) have also shown conservation of function (directing convergent extension movements) between the fish and human proteins. The membrane topology and associated secondary structure established here put in perspective a number of predicted structural and functional features of the protein. First, they demonstrate a cytoplasmic location for the C-terminal moiety of the protein, including the PDZ-binding motif (ETSV). This agrees with the previous observations made in intact proteins and with protein subdomains showing interactions of this C-terminal Vangl1/2 segment with the DIX subdomain of cytoplasmic PCP proteins Dvl1, Dvl2, and Dvl3.[28] The ETSV tetrapeptide has been shown to promote these interactions.[30,31] Second, this topology places membrane targeting and/or internalization motifs for clathrin-mediated endocytosis in the N-terminus ($YSFG_{7-10}$, $YSYY_{10-13}$, and LL_{56-57}) and in the C-terminus ($YKDF_{284-287}$ and $NPNL_{291-294}$) of the protein, where they would be expected to be functional. However, this topological model also suggests that predicted asparagine (N)-linked glycosylation sites NDS_{59-61} (N-terminus), $NST_{314-316}$, and $NNS_{317-319}$ (C-terminus) are unlikely to be functionally modified because they map to intracytoplasmic portions of the protein (Figure 6).

There are three available *loop*−*tail* (*Lp*) alleles for which loss-of-function mutations at *Vangl2* have been reported (D255E, R259L, and S464N). In humans, seven *VANGL2* mutations (S84F, R135W, R177H, L242V, T247M, R353C, and F437S) have been reported in neural tube defects, and so far, two of them have exhibited partial (R353C) or complete (F437S) loss of function expressed as the loss of the Vangl−Dvl interaction. On the other hand, eight *VANGL1* mutations (S83L, F153S, R181Q, L202F, V239I, R274Q, M328T, and A404S) have been detected in sporadic or familial cases of NTD, and two (M328T and V239I) are known to be complete loss-of-function mutants as shown by impairment of Vangl−Dvl interaction and loss of functional complementation in zebrafish.[32] Although the molecular mechanism underlying the defect of the other mutations remains unknown, a superimposition of the site of disease-associated VANGL variants on the structural model established points out interesting structure−function relationships (Figure 6). We note that of the 19 pathology-associated variants, five of them map to the membrane-associated portion of the proteins, including the loss-of-function $VANGL1^{V239I}$ allele detected as a de novo mutation in a familial case of NTD. Strikingly, we note the clustering of five additional such variants to a short 30-amino acid segment immediately downstream from TM4, including two *Lp*-associated mutations ($Vangl2^{D255E}$ and $Vangl2^{R259L}$). The clustering of L242F, T247M, and R274Q to this segment indirectly suggests that these variants may also be pathological. The functional role of this mutation-sensitive segment is unknown, but biochemical analysis of D255E, R259L, and $S467N^{27}$ shows that it is likely to be important for protein folding and membrane targeting. Finally, the remaining variants are distributed in the C-terminal cytoplasmic domain of the protein. Such variants may interfere with recruitment of other PCP proteins such as Dvl and Pk to Vangl, and these hypotheses can now be tested experimentally.

■ ASSOCIATED CONTENT

Ⓢ Supporting Information. TMHMM model predication of hVangl1 transmembrane helices and comparison with the TOPPRED2 model and immunofluorescence analysis of the

expression of HA-tagged Vangl1 proteins lacking the GFP tag (HA64, intracellular; HA139, extracellular). This material is available free of charge via the Internet at http://pubs.acs.org.

AUTHOR INFORMATION

Corresponding Author

*Department of Biochemistry, McGill University, 3649 Promenade Sir William Osler, Room 366, Montreal, Quebec, Canada H3G 0B1. Telephone: (514) 398-7291. Fax: (514) 598-2603. E-mail: philippe.gros@mcgill.ca.

Funding Sources

This work was supported by a research grant to P.G. from the Canadian Institutes of Health Research (MOP-13425). P.G. is a James McGill Professor of Biochemistry.

ACKNOWLEDGMENT

Image acquisition, data analysis, and image processing were conducted on equipment and with the assistance of the McGill Life Science Complex Imaging Facility, which was founded by the Canadian Foundation for Innovation.

ABBREVIATIONS

Lp, *loop*−*tail*; NTDs, neural tube defects; PCP, planar cell polarity; CE, convergent extension; Fz, Frizzled; Dgo, Diego; Fmi, Flamingo; Pk, Prickle; Dvl, Dishevelled; PBM, PDZ-binding motif; PM, plasma membrane.

REFERENCES

(1) Copp, A. J., Greene, N. D., and Murdoch, J. N. (2003) The genetic basis of mammalian neurulation. *Nat. Rev. Genet. 4*, 784–793.

(2) Harris, M. J., and Juriloff, D. M. (2007) Mouse mutants with neural tube closure defects and their role in understanding human neural tube defects. *Birth Defects Res., Part A 79*, 187–210.

(3) Bassuk, A. G., and Kibar, Z. (2009) Genetic basis of neural tube defects. *Semin. Pediatr. Neurol. 16*, 101–110.

(4) Strong, L. C., and Hollander, W. F. (1949) Hereditary loop-tail in the house mouse. *J. Hered. 40*, 329–334.

(5) Copp, A. J., and Greene, N. D. (2010) Genetics and development of neural tube defects. *J. Pathol. 220*, 217–230.

(6) Kibar, Z., Vogan, K. J., Groulx, N., Justice, M. J., Underhill, D. A., and Gros, P. (2001) Ltap, a mammalian homolog of *Drosophila Strabismus/Van Gogh*, is altered in the mouse neural tube mutant loop-tail. *Nat. Genet. 28*, 251–255.

(7) Murdoch, J. N., Doudney, K., Paternotte, C., Copp, A. J., and Stanier, P. (2001) Severe neural tube defects in the loop-tail mouse result from mutation of Lpp1, a novel gene involved in floor plate specification. *Hum. Mol. Genet. 10*, 2593–2601.

(8) Jessen, J. R., and Solnica-Krezel, L. (2004) Identification and developmental expression pattern of van gogh-like 1, a second zebrafish strabismus homologue. *Gene Expression Patterns 4*, 339–344.

(9) Torban, E., Wang, H. J., Patenaude, A. M., Riccomagno, M., Daniels, E., Epstein, D., and Gros, P. (2007) Tissue, cellular and subcellular localization of the Vangl2 protein during embryonic development: Effect of the Lp mutation. *Gene Expression Patterns 7*, 346–354.

(10) Torban, E., Patenaude, A. M., Leclerc, S., Rakowiecki, S., Gauthier, S., Andelfinger, G., Epstein, D. J., and Gros, P. (2008) Genetic interaction between members of the Vangl family causes neural tube defects in mice. *Proc. Natl. Acad. Sci. U.S.A. 105*, 3449–3454.

(11) Kibar, Z., Torban, E., McDearmid, J. R., Reynolds, A., Berghout, J., Mathieu, M., Kirillova, I., De Marco, P., Merello, E., Hayes, J. M., Wallingford, J. B., Drapeau, P., Capra, V., and Gros, P. (2007) Mutations in VANGL1 associated with neural-tube defects. *N. Engl. J. Med. 356*, 1432–1437.

(12) Kibar, Z., Bosoi, C. M., Kooistra, M., Salem, S., Finnell, R. H., De Marco, P., Merello, E., Bassuk, A. G., Capra, V., and Gros, P. (2009) Novel mutations in VANGL1 in neural tube defects. *Hum. Mutat. 30*, E706–E715.

(13) Kibar, Z., Salem, S., Bosoi, C. M., Pauwels, E., De Marco, P., Merello, E., Bassuk, A. G., Capra, V., and Gros, P. (2010) Contribution of VANGL2 mutations to isolated neural tube defects. *Clin. Genet.*.

(14) Lei, Y. P., Zhang, T., Li, H., Wu, B. L., Jin, L., and Wang, H. Y. (2010) VANGL2 mutations in human cranial neural-tube defects. *N. Engl. J. Med. 362*, 2232–2235.

(15) Fanto, M., and McNeill, H. (2004) Planar polarity from flies to vertebrates. *J. Cell Sci. 117*, 527–533.

(16) Roszko, I., Sawada, A., and Solnica-Krezel, L. (2009) Regulation of convergence and extension movements during vertebrate gastrulation by the Wnt/PCP pathway. *Semin. Cell Dev. Biol. 20*, 986–997.

(17) Bastock, R., Strutt, H., and Strutt, D. (2003) Strabismus is asymmetrically localised and binds to Prickle and Dishevelled during *Drosophila* planar polarity patterning. *Development 130*, 3007–3014.

(18) Strutt, H., and Strutt, D. (2009) Asymmetric localisation of planar polarity proteins: Mechanisms and consequences. *Semin. Cell Dev. Biol. 20*, 957–963.

(19) Montcouquiol, M., Sans, N., Huss, D., Kach, J., Dickman, J. D., Forge, A., Rachel, R. A., Copeland, N. G., Jenkins, N. A., Bogani, D., Murdoch, J., Warchol, M. E., Wenthold, R. J., and Kelley, M. W. (2006) Asymmetric localization of Vangl2 and Fz3 indicate novel mechanisms for planar cell polarity in mammals. *J. Neurosci. 26*, 5265–5275.

(20) Chacon-Heszele, M. F., and Chen, P. (2009) Mouse models for dissecting vertebrate planar cell polarity signaling in the inner ear. *Brain Res. 1277*, 130–140.

(21) Wang, J., Mark, S., Zhang, X., Qian, D., Yoo, S. J., Radde-Gallwitz, K., Zhang, Y., Lin, X., Collazo, A., Wynshaw-Boris, A., and Chen, P. (2005) Regulation of polarized extension and planar cell polarity in the cochlea by the vertebrate PCP pathway. *Nat. Genet. 37*, 980–985.

(22) Etheridge, S. L., Ray, S., Li, S., Hamblet, N. S., Lijam, N., Tsang, M., Greer, J., Kardos, N., Wang, J., Sussman, D. J., Chen, P., and Wynshaw-Boris, A. (2008) Murine dishevelled 3 functions in redundant pathways with dishevelled 1 and 2 in normal cardiac outflow tract, cochlea, and neural tube development. *PLoS Genet. 4*, e1000259.

(23) Curtin, J. A., Quint, E., Tsipouri, V., Arkell, R. M., Cattanach, B., Copp, A. J., Henderson, D. J., Spurr, N., Stanier, P., Fisher, E. M., Nolan, P. M., Steel, K. P., Brown, S. D., Gray, I. C., and Murdoch, J. N. (2003) Mutation of Celsr1 disrupts planar polarity of inner ear hair cells and causes severe neural tube defects in the mouse. *Curr. Biol. 13*, 1129–1133.

(24) Wang, Y., Guo, N., and Nathans, J. (2006) The role of Frizzled3 and Frizzled6 in neural tube closure and in the planar polarity of inner-ear sensory hair cells. *J. Neurosci. 26*, 2147–2156.

(25) Guo, N., Hawkins, C., and Nathans, J. (2004) Frizzled6 controls hair patterning in mice. *Proc. Natl. Acad. Sci. U.S.A. 101*, 9277–9281.

(26) Merte, J., Jensen, D., Wright, K., Sarsfield, S., Wang, Y., Schekman, R., and Ginty, D. D. (2010) Sec24b selectively sorts Vangl2 to regulate planar cell polarity during neural tube closure. *Nat. Cell Biol. 12*, 41–46, 47−48.

(27) Gravel, M., Iliescu, A., Horth, C., Apuzzo, S., and Gros, P. (2010) Molecular and cellular mechanisms underlying neural tube defects in the loop-tail mutant mouse. *Biochemistry 49*, 3445–3455.

(28) Torban, E., Wang, H. J., Groulx, N., and Gros, P. (2004) Independent mutations in mouse Vangl2 that cause neural tube defects in looptail mice impair interaction with members of the Dishevelled family. *J. Biol. Chem. 279*, 52703–52713.

(29) Czachorowski, M., Lam-Yuk-Tseung, S., Cellier, M., and Gros, P. (2009) Transmembrane topology of the mammalian Slc11a2 iron transporter. *Biochemistry 48*, 8422–8434.

(30) Saras, J., and Heldin, C. H. (1996) PDZ domains bind carboxy-terminal sequences of target proteins. *Trends Biochem. Sci. 21*, 455–458.

(31) Songyang, Z., Fanning, A. S., Fu, C., Xu, J., Marfatia, S. M., Chishti, A. H., Crompton, A., Chan, A. C., Anderson, J. M., and Cantley, L. C. (1997) Recognition of unique carboxyl-terminal motifs by distinct PDZ domains. *Science 275*, 73–77.

(32) Reynolds, A., McDearmid, J. R., Lachance, S., De Marco, P., Merello, E., Capra, V., Gros, P., Drapeau, P., and Kibar, Z. (2010) VANGL1 rare variants associated with neural tube defects affect convergent extension in zebrafish. *Mech. Dev. 127*, 385–392.